Towards Global Predictions of the Mode-1 Internal Tide

B. D. Dushaw

Applied Physics Laboratory, University of Washington, Seattle, Washington, USA.

B. D. Dushaw, Applied Physics Laboratory, University of Washington, 1013 Northeast 40th Street, Seattle, WA, 98105, USA. (dushaw@apl.washington.edu)

A frequency and wavenumber analysis of satellite altimetry data for mode-1 internal tides over the central North Pacific ocean shows that these waves retain their spatial coherence over the 3500 km distance between the Hawaiian Ridge and the Aleutians. The frequency-wavenumber tidal analysis resolves signals consistent with the dispersion relation for internal tides. Waves propagating northward from Hawaii reach the Aleutians, and waves propagating southward from the Aleutians reach Hawaii. The result is consistent with the conclusion that mode-1 internal tides are likely predictable over most regions of the world's oceans. Accounting for the effect of stratification on the surface expression of the waves, mode amplitude, a quantitity more directly related to tidal energy, was derived. The internal-tide waves experience little attenuation as they cross the North Pacific basin. The radiation of internal tides across ocean basins affects the spatial distribution of tidal energy available for ocean mixing.

1. Introduction

Recently, Dushaw et al. *[2001]* found that mode-1 internal tides were more predictable than previously appreciated. It appears likely that a significant aspect of oceanic variability, that associated with mode-1 internal tides, can be predicted over much of the world's oceans. This predictability should not be taken for granted. The amplitude and phase of internal tides have never been predicted at arbitrary points in space and time, although there have been hints of this property along altimeter tracks near topographic features such as the Hawaiian Ridge. There are numerous applications for predictions of internal tides, although, of course, these applications are scientific in nature and secondary to such applications as tidal predictions for navigation. We have only begun to exploit the ability to predict the mode-1 internal tides for oceanographic research.

Dushaw et al. *[2011]* used a combined frequency and wavenumber ($\omega - \mathbf{k}$) harmonic analysis to derive maps of internal-tide harmonic constants from TOPEX/Poseidon (T/P) and Jason measurements of sea-surface height (SSH). These harmonic constants gave surprisingly robust and accurate predictions of mode-1 internal-tides near the Hawaiian Ridge, to at least 40°N *[Dushaw et al. 1995; Rainville et al. 2009]*, and in the western North Atlantic *[Dushaw 2006; Dushaw et al. 2011]*. Predictions are limited to the first internal tide mode, since that mode has the dominant expression in sea surface height, a long wavelength ($\sim$150 km) and a fast phase speed ($\sim$ 3.5 m/s). The predictability of higher modes is unknown. The amplitude and phase of predictions derived from altimetry closely matched the time series of historical in situ measurements by acoustic tomography, even though some of the historical data was obtained a decade or more before the altimetry data used to make the prediction.

Developing accurate predictive models for the internal tide will likely be a long process, however. The comparisons described in detail by Dushaw et al. *[2011]* demonstrate that these predictions are possible. It is now a matter of (1) developing procedures to hone the robustness and accuracy of the predictions, and (2) determining the limitations of those predictions. The regions where internal tide estimates can be tested by tomographic data, the North Pacific and western North Atlantic, are fairly benign, with fairly weak surface currents and mesoscale variability. It may be, or indeed seems likely, that the predictability apparent in these regions will not be so good in other regions. From the global perspective, the task at hand is to assess the internal-tide predictability, try to adapt the model employed in the tidal analysis of SSH for the specific conditions of each region to best extract predictable internal tides, or to understand why the predictability fails.

Dushaw et al. *[2011]* focussed on the tidal analysis over regional areas to derive predictions in specific locations for comparing to the available in situ data. In this paper, the analysis is applied to the central North Pacific between the Hawaiian Ridge and the Aleutian Islands. The resulting maps show that the internal tide waves retain their coherence as they cross ocean basins. For these waves, the time scale associated with this 3500-km distance is about 12 days. In addition, after properly accounting for the effects of varying stratification and latitude on the sea-surface-height expression of the waves, the dissipation of the waves is shown to be remarkably weak.

2. Internal tide propagation between Hawaii and the Aleutians

As discussed by Dushaw et al. *[2011]*, applying an $\omega - \mathbf{k}$ analysis to satellite data over a relatively large area is problematic because it is difficult to formulate an adequate wavenumber model for large areas. Indeed, it is likely the wavenumber content is not stationary across large areas. To work around this issue, the large area between Hawaii and the Aleutians was divided into subdomains of $11{\times}11°$, each overlapping adjacent subdomains by $2°$. The $\omega - \mathbf{k}$ analysis was applied to each subdomain independently. The solution over the entire domain was then constructed by merging the results from each subdomain using a simple cosine taper over the $2°$ overlap (Fig. 1a). Ten years of T/P+Jason altimeter data were used for the analysis, together with tandem track data *[Dibarboure et al. 2009]*. To estimate just the waves emanating northward from the Hawaiian ridge, the tidal model for Figure 1a assumed waves propagating only in the generally northward direction. The tidal fit therefore excludes southward propagating waves. The $\omega - \mathbf{k}$ analysis obtains a solution consistent with only the assumed wavenumbers, and excludes variability not consistent with the internal tide dispersion relation, such as the mesoscale. For the M_2 tidal constituent, coherent waves radiating from Hawaii to the Aleutians and the Gulf of Alaska are apparent, giving a stark demonstration of the advantage of the $\omega - \mathbf{k}$ analysis. Zhao and Alford (2009) computed energy fluxes for northward and southward waves that showed internal-tide energy radiating across the North Pacific basin. Here, these waves have been resolved to the extent that it is apparent that internal-tide waves cross ocean basins without much attenuation or loss of coherence.

A similar tidal analysis using only southward propagating waves found internal tide waves that propagate from the Aleutian Islands to the Hawaiian Ridge (Fig. 1b). Waves generated at the Ridge and radiating southward are also apparent. An optimal tidal analysis includes wavenumbers in both directions (results not shown). The addition of both northward and southward propagating waves produces an internal-tide field characterized by ubiquitous standing waves *[Zhao and Alford 2009], [Zhao et al. 2009], [Dushaw et al. 2011]*. The existence of these standing waves in the central North Pacific, formed by the interference of waves from Hawaii and waves from Alaska, is a telling indicator of the temporal coherence of these waves, inasmuch as an interference pattern is particularly sensitive to the phase variations of the underlying waves.

3. Sea-surface height and stratification

Dushaw et al. *[2011]* showed that stratification has a large influence on the surface expression of the internal tide. The dependence of surface expression on stratification can be illustrated by calculating the mode-1 displacement modes using the 2009 World Ocean Atlas *[Antonov et al. 2010; Locarnini et al. 2010]* and assuming a constant internal displacement over the world's oceans (Fig. 2). The calculation assumed a flat-bottom ocean of 5500 m depth to determine the effects of stratification alone. A proper calculation of the relation between mode amplitude and SSH would be a solution for the modes using the local depth and stratification, followed by a normalization to ensure equal energy density of the modes for a unit mode-1 amplitude. The effects of varying depth and energy are small over most of the oceans, however, since the ocean basins have fairly constant depths of 5000-6000 m. In any case, it is apparent that for a given internal amplitude, the surface expression of internal tides in tropical latitudes is generally much greater than in higher latitudes. This effect has led to general conclusions concerning the decay properties of the internal (e.g., *Tian et al. [2008]*), but accounting for the effects of stratification changes notions of the decay of the internal tide considerably. Calculating internal displacement, more directly related to internal-tide energy density than SSH, shows that the mode-1 internal tide has a much larger decay scale that previously appreciated (Fig. 3). Indeed, for cases such as waves radiating northward from the Hawaiian Ridge, cylindrical spreading must also be accounted for when estimating a decay length scale.

4. Comments on the calculation of internal-tide energy flux

Although it is a common procedure (e.g., Ray and Cartwright *[2001]*, *Dushaw [2002]*, *Zhao and Alford [2009]*, calculating energy flux at single points of a field resulting from multiple interfering waves, or by fitting monochromatic plane waves, is problematic, if for no other reason than it provides an erroneous physical picture. For example, one of the reasons the Hawaiian Ocean Mixing Experiment (HOME) *[Pinkel et al. 2000; Carter et al. 2008; Rainville et al. 2009]* focussed on Kaena Ridge was because of the maps showing "beams" of internal-tide energy apparently emanating from there. It is now clear that much of the energy of those "beams" did not emanate from the Kaena Ridge. Rather, the "beams" are formed by the superposition of multiple waves emanating from a wide stretch of the Hawaiian Ridge *[Rainville et al. 2009, Zhao and Alford 2009]*. Also, the energy flux calculated based on the interference "beams" suggests a decay length scale that bears little resemblance to the actual decay scale of mode-1 internal tides. The energy flux derived from "beams" diminishes when the waves are no longer in constructive interference (c.f.,

Fig. 1a). Such “beams” do not have a real physical meaning, other than that the tidal amplitude there is large because of constructive interference (Fig. 4).

Two rigorous, equivalent approaches to estimating the mode-1 energy flux of complicated wave fields are proposed. The energy flux is fundamentally defined as $(\langle p'u'\rangle, \langle p'v'\rangle)$. In the context of the interference patterns of the internal tide around Hawaii, some care must be given to defining what is meant by the brackets $\langle\cdot\rangle$. This averaging implies an average over time to remove the oscillations of energy flux with time, an average over depth to remove the oscillations of energy flux with depth, and, by analogy, an average over area to remove the oscillations of energy flux with area. This latter average is most often omitted, giving the common figures of beams of large energy apparently emanating from such locations as the Kaena Ridge. Without the area average, expressions such as $\langle p'u'\rangle$, with p' and u' expanded as grand summations over frequency, mode, and wavenumber, retain cross terms of wavenumbers which have no clear physical meaning. With such averaging, the energy flux reduces to a simple summation of the square of the individual components, as required.

As an alternative to the averaging implied by the brackets, the variability can be separated in frequency, mode, and wavenumber (time, depth, and area) manually. A tidal analysis can separate the signals of the constituent frequencies, a modal decomposition can separate the signals of individual modes, and a wavenumber decomposition can separate the signals of individual wavenumbers. With this separation, no averaging $\langle\cdot\rangle$ is required, since the individual components of the tidal variability can be directly added. The frequency and wavenumber decompositions are a direct product of the $\omega - \mathbf{k}$ tidal analysis. The tidal signals derived from SSH discussed here are dominated by mode 1 and consistent with the mode-1 dispersion relation, giving a natural isolation of the first mode.

5. Discussion

Dushaw et al. *[2011]* concluded that the mode-1 internal tide is likely predictable, in the traditional tidal sense, over most regions of the world's oceans. Temporally incoherent contributions to mode-1 internal tides appeared to be minimal, at least in the North Pacific and western North Atlantic oceans, and the waves showed very little attenuation. Here, consistent with those conclusions, the mode-1 internal tides are found to have a spatial coherence that extends across the North Pacific basin. Further, after correcting for the effect of local stratification on the surface expression of the internal tides and allowing for cylindrical spreading, little decay of the mode-1 amplitude is evident over the 3500 km distance between the Hawaiian Ridge and the Aleutians.

One aim of this project is to provide accurate predictions of the internal-tide signatures of sea-surface height, so that this noise element may be removed from other observations such as satellite observations by the Surface Water and Ocean Topography (SWOT) mission. Such predictions also will require an assessment of their reliability, depending on the ocean region of interest. It seems unlikely that internal tides in all areas of the world's oceans will be as predictable as they seem to be in the North Pacific. A quantitative assessment of this predictability over the world's oceans is required. High-resolution models or state estimates such as are available from the Estimating the Circulation and Climate of the Ocean (ECCO2) program *[Menemenlis et al. 2008]* may give an accurate estimate for the environment through which internal tides propagate, hence may help identify the processes that disrupt internal-tide coherence (see also Arbic et al. *[2010]*). Including all tidal constituents, the signals of internal tides in SSH have typical amplitudes of $3-5$ cm in most regions of the ocean.

Unlike the basic premise of HOME, the tidal energy budget and its relation to deep-ocean mixing is not a local problem. Internal tide waves that carry most of the energy lost from the barotropic tide *[Carter et al. 2008]* at any location can cross ocean basins with little dissipation to deposit their energy on distant coastlines. Meanwhile, even at remote locations such as the Hawaiian Ridge, radiated internal-tide energy can arrive from distant regions. When it arrives at coastlines or shoaling topography, internal-tide energy either dissipates or reflects. These energy considerations determine the spatial distribution of tidally-driven deep ocean mixing, an essential aspect of general circulation models.

Acknowledgments. This project was initially supported by grant OCE-0647743 from the National Science Foundation.

References

Arbic, B. K., and A. J. Wallcraft and E. J. Metzger (2010), Concurrent simulation of the eddying general circulation and tides in a global ocean model, *Ocean Modelling*, *32*, 175–187, doi:10.1016/j.ocemod.2010.01.007.

Antonov, J. I., D. Seidov, T. P. Boyer, R. A. Locarnini, A. V. Mishonov, H. E. Garcia, O. K. Baranova, M. M. Zweng, and D. R. Johnson (2010), *World Ocean Atlas 2009, Volume 2: Salinity.* S. Levitus, Ed. NOAA Atlas NESDIS 69, U.S. Government Printing

Office, Washington, D.C., 184 pp.

Carter, G. S., M. A. Merrifield, J. M. Becker, K. Katsumata, M. C. Gregg, D. S. Luther, M. D. Levine, T. J. Boyd, and Y. L. Firing (2008), Energetics of M_2 Barotropic-to-Baroclinic Tidal Conversion at the Hawaiian Islands, *J. Phys. Oceanogr.*, *38*, 2205–2223.

Dibarboure, G. and O. Lauret and F. Mertz and V. Rosmorduc and C. Maheu (2009), SSALTO/DUACS User Handbook: (M)SLA and (M)ADT Near-Real Time and Delayed Products, AVISO Altimetry, CLS-DOS-NT-06.034, Issue 1.10, SALP-MU-P-EA-21065-CLS, March 4, 2009, 41 pp.

Dushaw, B. D. (2006), Mode-1 internal tides in the western North Atlantic Ocean, *Deep Sea Res. I*, *53*, 449–473.

Dushaw, B. D., P. F. Worcester, and M. A. Dzieciuch (2011), On the predictability of mode-1 internal tides, *Deep Sea Res. I*, *58*, 677–698, doi:10.1016/j.dsr.2011.04.002.

Dushaw, B. D., P. F. Worcester, B. D. Cornuelle, B. M. Howe, and D. S. Luther, 1995. Baroclinic and barotropic tides in the central North Pacific Ocean determined from long-range reciprocal acoustic transmissions. *J. Phys. Oceanogr.*, *25*, 631–647.

Locarnini, R. A., A. V. Mishonov, J. I. Antonov, T. P. Boyer, H. E. Garcia, O. K. Baranova, M. M. Zweng, and D. R. Johnson (2010), *World Ocean Atlas 2009, Volume 1: Temperature*. S. Levitus, Ed. NOAA Atlas NESDIS 68, U.S. Government Printing Office, Washington, D.C., 184 pp.

Menemenlis, D., J. Campin, P. Heimbach, C. Hill, T. Lee, A. Nguyen, M. Schodlock, and H. Zhang (2008), ECCO2: High resolution global ocean and sea ice data synthesis, *Mercator Ocean Quarterly Newsletter*, *31*, 13–21.

Pinkel, R., W. Munk, P. Worcester, B. D. Cornuelle, D. Rudnick, J. Sherman, J. H. Filloux, B. D. Dushaw, B. M. Howe, T. B. Sanford, C. M. Lee, E. Kunze, M. C. Gregg, J. B. Miller, J. M. Moum, D. R. Caldwell, M. D. Levine, T. Boyd, G. D. Egbert, M. A. Merrifield, D. S. Luther, E. Firing, R. Brainard, P. J. Flament, and A. D. Chave (2000), Ocean mixing studied near Hawaiian Ridge, *Eos, Trans. Am. Geophys. U.*, *81*, 545,553.

Rainville, L., T. M. Shaun Johnston, G. S. Carter, M. A. Merrifield, R. Pinkel, B. D. Dushaw, P. F. Worcester (2009), Interference pattern and propagation of the M_2 internal tide south of the Hawaiian Ridge, *J. Phys. Oceanogr.*, *40*, 311–325. doi 10.1175/2009JPO4256.1

Ray, R. D., and D. E. Cartwright (2001), Estimates of internal tide energy fluxes from Topex/Poseidon altimetry: Central North Pacific, *Geophys. Res. Lett.*, *28*, 1259–1263.

Zhao, Z., and M. H. Alford (2009), New altimetric estimates of mode-1 M_2 internal tides in the North Pacific Ocean, *J. Phys. Oceanogr.*, *39*, 1669–1684, doi:10.1175/2009JPO3922.1.

Zhao, Z., M. H. Alford, J. A. MacKinnon, R. Pinkel (2010), Long-Range Propagation of the Semidiurnal Internal Tide from the Hawaiian Ridge. *J. Phys. Oceanogr.*, *40*, 713–736, doi:10.1175/2009JPO4207.1.

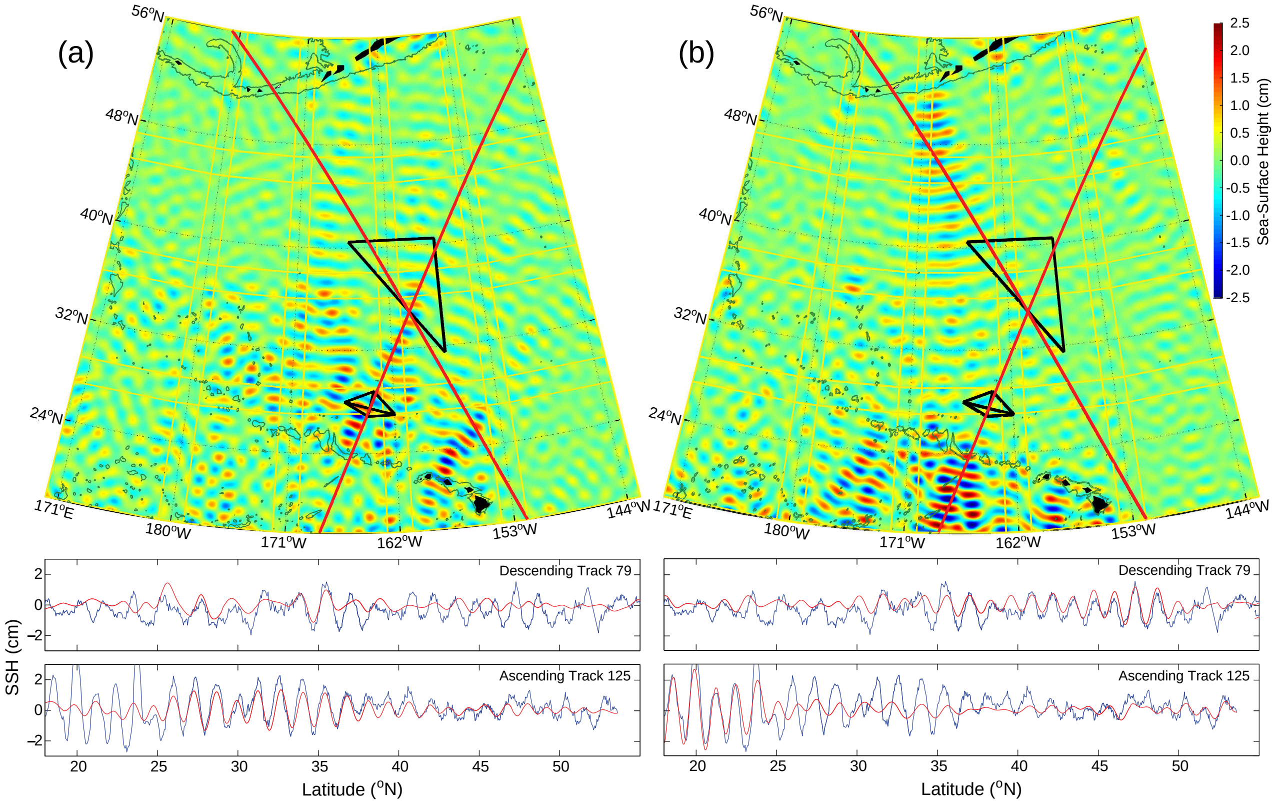

Figure 1. (a) The cosine component of the harmonic constants (A cos(G)) for the M_2, mode-1 internal tide derived from a $\omega - \mathbf{k}$ analysis of T/P+Jason SSH assuming wavenumbers in the northward direction. The discrete yellow lines indicate the boundaries of the independent subdomains, overlapping by 2°. The RTE87 triangle *[Dushaw et al. 1995]* and HOME diamond tomography arrays *[Rainville et al. 2009]* are indicated. (b) Assuming wavenumbers of general southward direction. Lambert azimuthal equal area projection. (Bottom panels) Comparison of point-wise (blue) and $\omega - \mathbf{k}$ (red) harmonic constants along tracks 79 and 125, indicated by the red lines on the top maps.

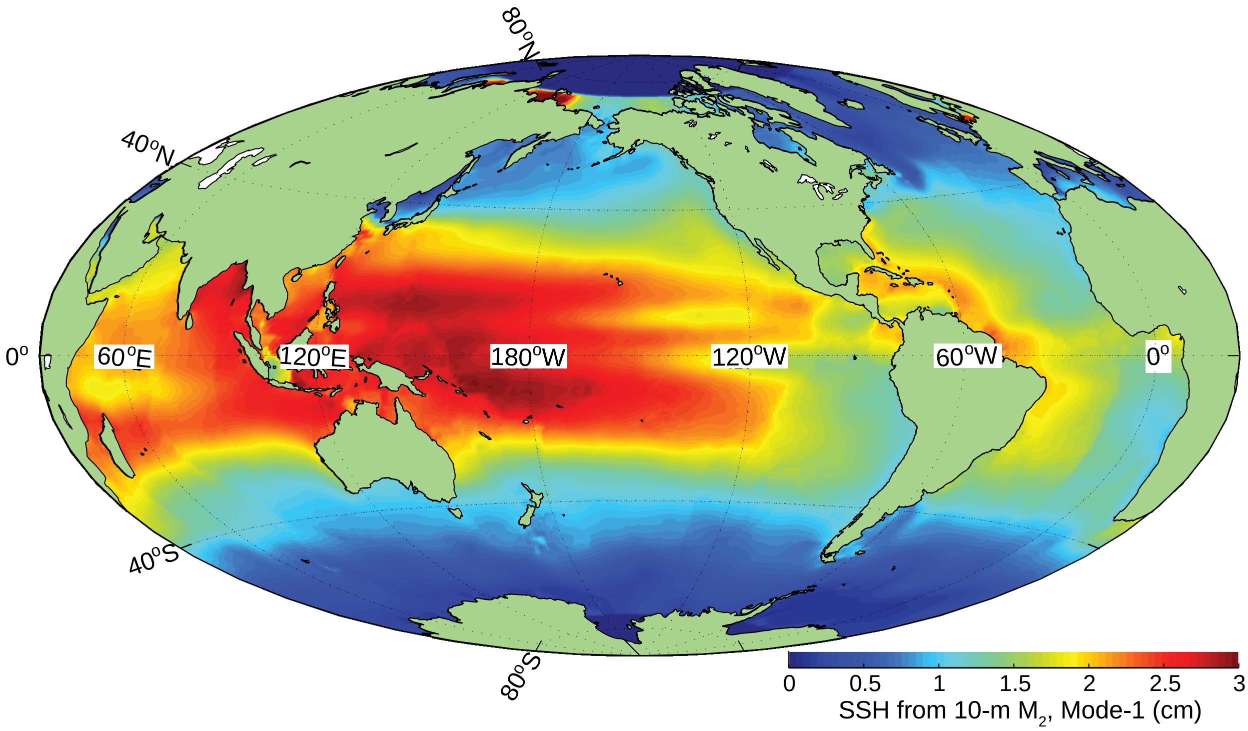

Figure 2. Amplitude of SSH in cm of a mode-1 internal tide at M_2 frequency with 10-m internal displacement amplitude over the world's oceans derived from the 2009 World Ocean Atlas. The surface expression of the internal tide depends on the local stratification, hence local conditions must be accounted for when calculating energy or mode amplitude from a measurement of SSH.

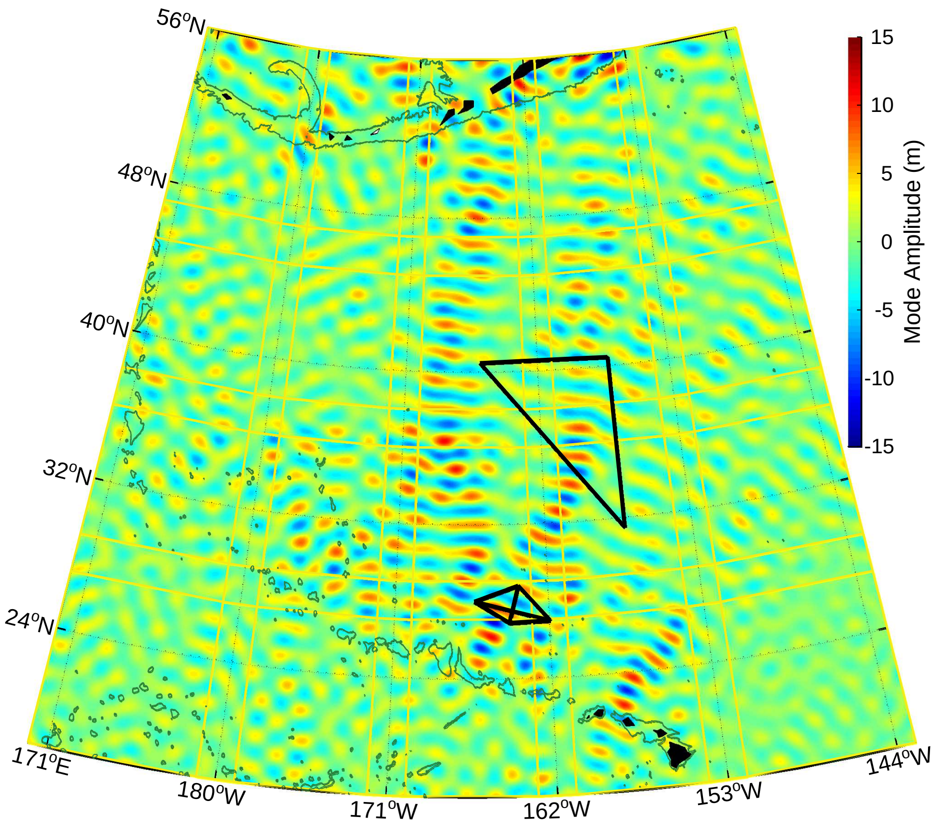

Figure 3. The mode amplitude derived from the map of SSH assuming northward wavenumbers (Fig. 1a). Internal tides experience quite weak decay as they propagate across ocean basins. With the mode function normalization employed here, "Mode Amplitude" is roughly equal to the maximum internal displacement of the mode in meters.

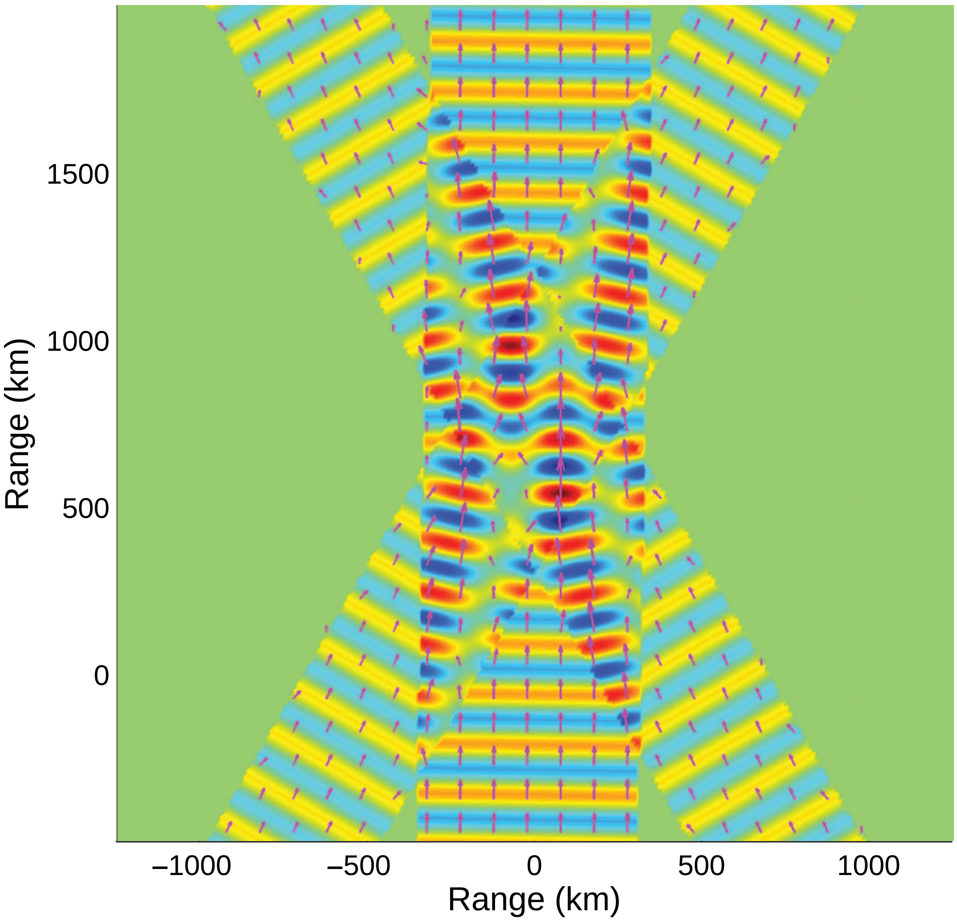

Figure 4. Simple illustration of the problem of deriving point-wise energy flux vectors from a field comprised of interfering waves. Where these waves form a complicated interference pattern at their intersection, a complicated field of energy flux vectors is obtained. In this case, there are only three energy flux vectors, one for each monochromatic wave.